CONFIDENTIAL

Copy 286
RM L54C17

NACA RM L54C17

NACA

RESEARCH MEMORANDUM

FLIGHT DETERMINATION OF THE BUFFETING CHARACTERISTICS OF THE BELL X-5 RESEARCH AIRPLANE AT 58.7° SWEEPBACK

By Donald W. Briggs

Langley Aeronautical Laboratory
Langley Field, Va.

CLASSIFIED DOCUMENT

NATIONAL ADVISORY COMMITTEE
FOR AERONAUTICS

WASHINGTON

May 24, 1954

CONFIDENTIAL

NATIONAL ADVISORY COMMITTEE FOR AERONAUTICS

RESEARCH MEMORANDUM

FLIGHT DETERMINATION OF THE BUFFETING CHARACTERISTICS OF THE BELL X-5 RESEARCH AIRPLANE AT 58.7° SWEEPBACK

By Donald W. Briggs

SUMMARY

Flight measurements were made of the buffeting characteristics of the Bell X-5 research airplane at 58.7° sweepback in the Mach number range from 0.65 to approximately 1.03 at altitudes from 37,000 to 43,000 feet. Maximum airplane normal-force coefficients were attained for Mach numbers up to 0.96.

At all airplane normal-force coefficients the horizontal tail was found to experience buffeting. An increase in tail buffeting intensity occurred essentially simultaneously with the break in the airplane normal-force coefficient—angle-of-attack curve. At angles of attack below maximum airplane normal-force coefficient the peak buffet-induced tail bending stresses were 20 percent of the maximum observed tail steady-state bending stress; the peak buffet-induced tail shear loads were approximately 5 percent of the tail design limit load.

Wing buffeting began at moderate angles of attack but above the wing buffet boundary there was no appreciable increase in wing buffet intensity with increase in Mach number or angle of attack. At angles of attack below maximum airplane normal-force coefficient, the peak buffet-induced wing bending stresses were 5 percent of the maximum observed wing steady-state bending stress.

Coefficients of incremental normal acceleration greater than ±0.05, considered to be high-intensity buffeting on other research airplanes, were not experienced by the X-5 airplane below maximum airplane normal-force coefficient. The pilot considered the buffeting to be "unobjectionable" throughout the entire test region.

INTRODUCTION

As part of the joint Air Force—Navy—NACA research program, the Bell X-5 research airplane was obtained for the National Advisory Committee for Aeronautics for investigation in flight of the effects of large variations in wing sweep angle. After completion of acceptance tests, the results of which are presented in reference 1, the NACA High-Speed Flight Research Station at Edwards Air Force Base, Calif., initiated a program to investigate the stability and control characteristics of the airplane at 58.7° sweepback. During this program an investigation of the buffeting characteristics of the airplane was also conducted. Most of the buffet data obtained consisted of measurements made of buffet-induced wing and tail bending stresses and of the buffet-induced increments in normal acceleration at the airplane center of gravity. Near the completion of the test program at 58.7°, the tail stress measurements were discontinued and measurements of buffet-induced increments in horizontal tail shear load, bending moment, and torque were made. The results of these various buffet measurements are presented in this paper.

SYMBOLS

a_n	normal acceleration at airplane center of gravity, g units
C_{N_A}	airplane normal-force coefficient, nW/qS
c	chord, ft
g	acceleration due to gravity, ft/sec^2
h_p	pressure altitude, ft
M	Mach number
n	airplane normal load factor
q	dynamic pressure, lb/sq ft
S	wing area, sq ft
W	airplane weight, lb
α	airplane angle of attack, deg

Δa_n	buffet-induced increment in normal acceleration at airplane center of gravity, ±g units
ΔBM	buffet-induced increment in horizontal tail structural bending moment, ±in-lb
ΔC_{a_n}	incremental coefficient of normal acceleration due to buffeting, $W\Delta a_n/qS$
ΔT	buffet-induced increment in horizontal tail structural torque about 57-percent-chord line of strain-gage station, ±in-lb
ΔV	buffet-induced increment in shear load on one side of horizontal tail, ±lb
$\Delta\sigma$	buffet-induced increment in bending stress, ±lb/sq in.

Subscripts:

max	maximum
T	horizontal tail
W	wing

INSTRUMENTATION

Standard NACA instruments, synchronized by a common timer, recorded most of the quantities pertinent to this investigation.

The airspeed system was calibrated by the "fly-by" method up to a Mach number of 0.70 and by the radar phototheodolite method (ref. 2) at Mach numbers greater than 0.70. The accuracy of the Mach numbers obtained from the airspeed calibration is within ±0.01.

Angle of attack was measured with a vane mounted on a nose boom projecting from above the air inlet duct. The vane was mounted approximately 51 inches forward of the nose boom-fuselage juncture (fig. 1). The recorded angles of attack were uncorrected for upwash or bending of the boom. The recorded position of the angle-of-attack vane is accurate to within ±0.2°.

The airplane is instrumented with four-arm strain-gage bridges located at several chordwise positions near the roots of the wing and tail. During most of the flight test program the outputs of each

strain-gage bridge were photographically recorded as separate traces. The strain gages on each structural component were statically calibrated in terms of shear load, bending moment, and torque by the method of reference 3.

The buffet-induced increments in horizontal tail bending stress presented in this paper were determined from the response of one strain-gage bridge with arms located on the upper and lower inner-skin surfaces near the root of the left side of the horizontal tail. The increments in wing bending stress were measured with a similar type strain-gage bridge mounted on the web of the wing main beam near the wing-fuselage juncture.

During the portion of the tests in which the output of each individual strain-gage bridge was recorded, steady loads were measured by mathematically combining the several bridge outputs into the load equations determined during the strain-gage calibration. This procedure could not be used to determine buffet loads, however, because of the difficulty in determining the proper phase relationships between the output fluctuations of the several bridges utilized in each load equation. During the latter part of the program, therefore, the outputs of the several bridges utilized in each horizontal tail load equation were electrically combined such that shear load, bending moment, and torque were recorded as individual traces by the oscillograph. During buffeting, the amplitude of the fluctuations of each trace was directly proportional to the magnitude of the buffet quantity.

Incremental tail shear load was measured on both the right and left sides of the horizontal tail. Incremental bending moment was measured on the left side of the horizontal tail with the strain-gage station (at a chordwise station 14.5 inches outboard of the airplane line of symmetry) as the bending-moment axis. The increments in torque were measured for the right side of the tail about an axis perpendicular to the strain-gage station and running through the 57-percent-chord line of the gage station.

The accuracy of the strain-gage calibration is as follows:

Shear load, right side, percent	3
Shear load, left side, percent	3
Bending moment, left side, percent	13
Torque, right side, percent	15

Buffet-induced loads on the wing were not measured during these tests and because of the electrical combination of the tail gages, tail stresses and tail loads could not be measured simultaneously.

The output of all strain-gage bridges, combined and uncombined, was recorded with a 36-channel Consolidated recording oscillograph which has a frequency response flat to at least 60 cycles per second.

Incremental fluctuations in normal acceleration at the airplane center of gravity were obtained with an air-damped accelerometer having a natural frequency of 13.5 cycles per second. The dynamic response of the instrument during flight was corrected for variations in air density by using the results of a ground calibration of the variation of damping with air density. The predominant frequency of the buffet-induced fluctuations in normal acceleration (with respect to both amplitude and occurrence) was measured to be 13 to 14 cycles per second. The recorded dynamic amplitudes were corrected for frequency response using 13.5 cycles per second as the average forcing frequency.

All buffet-induced quantities presented in this paper have been taken as plus-or-minus fluctuations of the quantity about its mean steady-state value.

AIRPLANE

The Bell X-5 airplane is a single-place fighter-type airplane powered by one Allison J-35-A-17 turbojet engine and is designed for research in the transonic speed range. The airplane incorporates a wing whose sweepback may be varied in flight between 20° and 58.7°. Full-span leading-edge wing slats are electrically operated and can be set at any desired position between fully closed and fully open. The incidence of the horizontal tail is variable. With the wing at the 58.7° sweepback position, the horizontal tail is located approximately 1.88 wing semispans behind the quarter chord of the wing mean aerodynamic chord and 0.135 wing semispan above the extended wing chord plane.

A three-view drawing of the airplane at 58.7° sweepback is shown in figure 1 and a photograph of the airplane in this configuration is shown in figure 2. Table I contains the pertinent physical characteristics and dimensions of the airplane at 58.7° sweepback. Horizontal tail, wing, and fuselage modes of vibration listed in table II are taken from unpublished results of ground vibration tests of the airplane.

TESTS

All data presented in this paper were obtained at altitudes from 37,000 to 43,000 feet in the Mach number range from 0.65 to about 1.03. Maximum airplane normal-force coefficient $C_{N_{A_{max}}}$, defined for these

tests as the airplane normal-force coefficient C_{N_A} beyond which C_{N_A} decreases with increase in angle of attack, was reached for Mach numbers up to 0.96.

Data were taken from maneuvers performed in the clean configuration, slats closed, 100-percent engine rpm, and at a wing sweepback angle of 58.7°. Airplane weight during the tests varied from 9132 pounds to 8315 pounds and center-of-gravity position varied from 44.6 to 45.1 percent wing mean aerodynamic chord. The maneuvers consisted of elevator- or stabilizer-executed pull-ups, elevator-executed push-overs, and a limited number of level-flight speed runs. No appreciable difference in the buffeting characteristics was found between the elevator- and stabilizer-executed maneuvers.

Inasmuch as at moderate lift coefficients the airplane experienced a reduction of longitudinal stability (ref. 4) followed by directional instability and aileron over-balance, the maneuvers did not extend over long periods of time above the boundary for reduction of longitudinal stability. Data obtained during the recovery portion of the maneuvers are not presented in this paper.

RESULTS AND DISCUSSION

General Buffeting Characteristics

Representative buffet data obtained during typical push-over and pull-up maneuvers are shown in figures 3 and 4. The data are shown for angles of attack up to the peak attained during each maneuver.

As indicated by the values of buffet-induced increments in tail bending stress $\Delta\sigma_T$ (fig. 3) and the buffet-induced tail loads (fig. 4) the horizontal tail experiences buffeting at all airplane normal-force coefficients.

Figures 3(a) and 3(b) and figures 4(a), 4(b), and 4(c) are typical of the tail buffeting experienced at Mach numbers below 0.90. The buffet-induced bending stresses $\Delta\sigma_T$ and shear loads ΔV show only a gradual increase with increasing angle of attack. In contrast, figures 3(c), 3(d), and 4(d), which are typical of the tail buffeting at Mach numbers from 0.90 to the highest reached during the tests, show the tail buffet magnitudes to first decrease then increase with increasing angle of attack. At all Mach numbers the increase in $\Delta\sigma_T$ and ΔV began near the angle of attack at which the airplane normal-force coefficient - angle-of-attack curve first became nonlinear. The increments in bending moment ΔBM and torque ΔT show essentially the same trends as the increments in bending stress and shear load.

The buffet-induced increments in wing bending stress $\Delta\sigma_W$ (fig. 3) show that wing buffeting begins at moderate angles of attack but that there is little increase in intensity as angle of attack and Mach number are increased.

The reflection at the airplane center of gravity of the tail and wing buffeting is indicated in the values of incremental fluctuations of normal acceleration Δa_n in figure 3. At angles of attack below that for start of wing buffeting, the values of Δa_n result solely from tail buffeting. Near the angle of attack for the start of wing buffeting, however, the values of Δa_n increase and it appears that wing buffeting contributes more to the increase in the fluctuations at the airplane center of gravity than is indicated by the magnitudes of the buffet-induced wing stresses.

Buffet Frequencies

The horizontal tail, wing, and airplane center of gravity buffeted at predominant frequencies of 16 to 18, 11 to 12, and 13 to 14 cycles per second, respectively.

Higher frequencies existed on the wing and tail strain-gage records but with the exception of the tail shear stress and shear loads records, the higher frequency fluctuations were of negligible amplitude. The records of both tail shear stress and shear load generally fluctuated simultaneously at frequencies of 16 to 18 and 80 cycles per second with the fluctuations at both frequencies being about equal in amplitude.

The predominant tail buffet frequency of 16 to 18 cycles per second is near that corresponding to the mode of stabilizer rocking coupled with fuselage torsion and fin bending, 15.9 cycles per second. (See table II for complete ground vibration test results.)

The fluctuations at 80 cycles per second noted on the tail shear traces correspond closely to the mode of first antisymmetrical stabilizer torsion (79.1 cps). The natural frequency for the first mode of symmetrical wing bending (10.3 cps) is near the 11 to 12 cycle-per-second range noted above as being the predominant wing buffet frequency.

The predominant frequency at which buffet-induced increments in normal acceleration were measured (13 to 14 cps) does not agree with any of the natural structural frequencies quoted for the fuselage in table II but does fall close to the resonant frequency of the instrument. Also, the data of table II are for the airplane in an empty-weight condition. During the flight tests the weight of the airplane was from 500 to 1300 pounds greater than the empty weight with most of

the weight difference arising from the fuel, all of which is carried inside the fuselage.

Buffet Magnitudes

The magnitudes of the buffet-induced increments in tail bending stress, shear load, bending moment, and torque experienced throughout the speed and lift range of the airplane at approximately 40,000 feet are summarized in figure 5. The curves for 1g, 2g, and 3g flight at 40,000 feet, together with the boundary for $C_{N_{A_{max}}}$, are also shown in these figures. It will be noted that the test limits differ for some of the data shown. This difference is due to the different number of flights for which data were available. The summary of the buffet-induced shear loads in figure 5(b) is shown for the right side of the horizontal tail only since both sides of the tail show essentially identical variations in buffet magnitudes (fig. 4).

Each of the summary figures (fig. 5) shows that for Mach numbers up to approximately 0.90 there is a large range of airplane normal-force coefficients in which the tail buffet intensity remains at a minimum value. In figure 5(a), for example, the buffet-induced tail bending stresses do not exceed ±100 pounds per square inch over most of the operational region. However, as $C_{N_{A_{max}}}$ is approached the intensity of buffeting increases. The airplane normal-force coefficients and angles of attack at which the increase in tail bending stresses occurred and at which the break in the C_{N_A}—α curve occurred are summarized in figure 6 for the Mach number range tested. It can be seen that the increase in tail buffeting occurs essentially simultaneously with the break in the C_{N_A}—α curve.

In addition to the increase in tail buffeting near $C_{N_{A_{max}}}$ noted in figure 5, the tail of the X-5 airplane also experiences an increase in buffeting at all airplane normal-force coefficients as the Mach number is increased above 0.90. This increase is most apparent at high and low values of C_{N_A} where buffeting of the largest magnitude was experienced. The data of figure 5 show that the tail buffeting begins to decrease at Mach numbers above approximately 0.96.

The design limit stress for the tail location at which tail buffet stresses were measured is not known. The peak steady-state stress occurring at this location during the flight tests, however, was 3960 pounds per square inch resulting from a load on the left stabilizer

of 1319 pounds. In the high lift region above $M = 0.90$ the peak tail buffet stresses were on the order of 20 percent of this peak steady-state stress.

The peak buffet-induced shear load ΔV on one side of the horizontal tail was measured to be ±200 pounds. The design limit load for one side of the X-5 horizontal tail is 3865 pounds. This peak value of ΔV is then approximately 5 percent of the design limit load.

Figure 7 shows the location of the wing buffet boundary throughout the Mach number range. Although there is a considerable range of lift between the wing buffet boundary and $C_{N_{A_{max}}}$, the data of figure 3 show that above the wing buffet boundary there was no appreciable variation of $\Delta\sigma_W$ with either increasing Mach number or angle of attack. Below $C_{N_{A_{max}}}$ the peak values of $\Delta\sigma_W$ were on the order of ±100 pounds per square inch. The maximum steady-state wing bending stress at the wing main beam - fuselage juncture was 2135 pounds per square inch, resulting from a maximum wing steady load of 9765 pounds. The maximum values of the buffet-induced wing bending stresses were then approximately 5 percent of the peak steady stress.

The buffet-induced increments in normal acceleration at the airplane center of gravity Δa_n increased gradually with lift throughout the Mach number range tested (fig. 3) but did not exceed ±0.2g at airplane normal-force coefficients up to about 0.07 below $C_{N_{A_{max}}}$. Near and at $C_{N_{A_{max}}}$ the values of Δa_n increased from ±0.2g but did not exceed ±0.45g.

Increments in the coefficient of buffet-induced normal acceleration ΔC_{a_n} of ±0.05, considered as high intensity buffeting on other research airplanes (refs. 5 and 6) were not experienced by the X-5 airplane below $C_{N_{A_{max}}}$ at any Mach number tested.

Buffeting Above $C_{N_{A_{max}}}$

On a number of flights angles of attack as high as 5° above that for $C_{N_{A_{max}}}$ were attained. The buffeting encountered at these angles of attack was higher in magnitude than that existing below $C_{N_{A_{max}}}$. The peak buffet-induced tail bending stresses increased to about 30 percent of the peak steady-state stress of 3960 pounds per square inch mentioned above. Tail buffet loads data were not obtained above $C_{N_{A_{max}}}$.

The buffet-induced stresses on the wing increased to approximately 10 percent of the peak steady-state wing stress of 2135 pounds per square inch. The peak buffet-induced fluctuations in normal acceleration observed above $C_{N_{A_{max}}}$ were approximately ±0.5g, or ±0.05g greater than the peak values of Δa_n experienced below $C_{N_{A_{max}}}$.

Pilot's Opinion

The pilot considers the buffeting experienced by the X-5 airplane to be "unobjectionable" throughout the region of the tests. In level flight the pilot reported the buffeting as first becoming "noticeable" (but still unobjectionable) at Mach numbers above 0.90 to 0.92. The data of figure 5 show that in 1g flight it is in the range from M = 0.90 to 0.92 that tail buffet magnitudes show their first indications of increasing from one level to a higher level.

CONCLUDING REMARKS

Flight measurements were made of the buffeting characteristics of the Bell X-5 research airplane at 58.7° sweepback in the Mach number range from 0.65 to approximately 1.03 at altitudes from 37,000 to 43,000 feet. Maximum airplane normal-force coefficients were attained for Mach numbers up to 0.96.

At all airplane normal-force coefficients the horizontal tail was found to experience buffeting. An increase in tail buffeting intensity occurred essentially simultaneously with the break in the airplane normal-force coefficient - angle-of-attack curve. At angles of attack below maximum airplane normal-force coefficient the peak buffet-induced tail bending stresses were 20 percent of the maximum observed tail steady-state bending stress; the peak buffet-induced tail shear loads were approximately 5 percent of the tail design limit load.

Wing buffeting began at moderate angles of attack but above the wing buffet boundary there was no appreciable increase in wing buffet intensity with increase in Mach number or angle of attack. At angles of attack below maximum airplane normal-force coefficient, the peak buffet-induced wing bending stresses were 5 percent of the maximum observed wing steady-state bending stress.

Coefficients of incremental normal acceleration greater than ±0.05, considered to be high-intensity buffeting on other research airplanes,

were not experienced by the X-5 airplane below maximum airplane normal-force coefficient. The pilot considered the buffeting to be "unobjectionable" throughout the entire test region.

Langley Aeronautical Laboratory,
National Advisory Committee for Aeronautics,
Langley Field, Va., March 2, 1954.

REFERENCES

1. Finch, Thomas W., and Briggs, Donald W.: Preliminary Results of Stability and Control Investigation of the Bell X-5 Research Airplane. NACA RM L52K18b, 1953.

2. Zalovcik, John A.: A Radar Method of Calibrating Airspeed Installations on Airplanes in Maneuvers at High Altitudes and at Transonic and Supersonic Speeds. NACA Rep. 985, 1950. (Supersedes NACA TN 1979.)

3. Skopinski, T. H., Aiken, William S., Jr., and Huston, Wilber B.: Calibration of Strain-Gage Installations in Aircraft Structures for the Measurement of Flight Loads. NACA TN 2993, 1953. (Supersedes NACA RM L52G31.)

4. Finch, Thomas W., and Walker, Joseph A.: Flight Determination of the Static Longitudinal Stability Boundaries of the Bell X-5 Research Airplane with 59° Sweepback. NACA RM L53A09b, 1953.

5. Baker, Thomas F.: Some Measurements of Buffeting Encountered by a Douglas D-558-II Research Airplane in the Mach Number Range from 0.5 to 0.95. NACA RM L53I17, 1953.

6. Baker, Thomas F.: Results of Measurements of Maximum Lift and Buffeting Intensities Obtained During Flight Investigation of the Northrop X-4 Research Airplane. NACA RM L53G06, 1953.

TABLE I.- PHYSICAL CHARACTERISTICS OF BELL X-5 AIRPLANE

AT A SWEEP ANGLE OF 58.7°

Airplane:	
Weight, lb:	
Full fuel	9976
Less fuel	7864
Power plant:	
Axial-flow turbojet engine	J-35-A-17
Center-of-gravity position, percent M.A.C.:	
Full fuel	45.0
Less fuel	45.5
Moments of inertia for 58.7° sweep (clean configuration-full fuel), slug-ft^2:	
About Y-axis	9495
About Z-axis	8040
Over-all height, ft	12.2
Over-all length, ft	33.6
Wing:	
Airfoil section (perpendicular to 38.02-percent-chord line):	
Root	NACA $64_{(10)}$A011
Tip	NACA $64_{(08)}$A008.28
Sweep angle at 0.25 chord, deg	58.7
Area, sq ft	183.7
Span, ft	20.05
Span between equivalent tips, ft	19.3
Aspect ratio	2.20
Taper ratio	0.411
Mean aerodynamic chord, ft	9.95
Location of leading edge of mean aerodynamic chord, fuselage station	101.2
Incidence root chord, deg	0
Dihedral, deg	0
Geometric twist, deg	0
Wing flaps (split):	
Area, sq ft	15.9
Span, parallel to hinge center line, ft	6.53
Chord, parallel to line of symmetry at 20° sweepback, in.:	
Root	30.8
Tip	19.2
Travel, deg	60

TABLE I.- PHYSICAL CHARACTERISTICS OF BELL X-5 AIRPLANE

AT A SWEEP ANGLE OF 58.7° - Continued

Slats (leading edge divided):	
Area, sq ft	14.6
Span, parallel to leading edge, ft	10.3
Chord, perpendicular to leading edge, in.:	
Root	11.1
Tip	6.6
Travel, percent wing chord:	
Forward	10
Down	5
Aileron (45 percent internal-seal pressure balance):	
Area (each aileron behind hinge line), sq ft	3.62
Span parallel to hinge center line, ft	5.15
Travel, deg	±15
Chord, percent wing chord	19.7
Moment area rearward of hinge line (total), $in.^3$	4380
Wing panel:	
Area, sq ft	113.62
Span, ft	14.33
Mean aerodynamic chord, ft	8.43
Location of leading edge of mean aerodynamic chord, fuselage station	138.6
Horizontal tail:	
Airfoil section (parallel to fuselage center line)	NACA 65A006
Area, sq ft	31.5
Span, ft	9.56
Aspect ratio	2.9
Sweep angle at 0.25-percent chord, deg	45
Mean aerodynamic chord, in.	42.8
Position of 0.25 mean aerodynamic chord, fuselage station	355.6
Stabilizer travel, (power actuated), deg:	
Leading edge up	4.5
Leading edge down	7.5
Elevator (20.8 percent overhang balance, 31.5 percent span):	
Area rearward of hinge line, sq ft	6.9
Travel from stabilizer, deg:	
Up	25
Down	20
Chord, percent horizontal tail chord	30
Moment area rearward of hinge line (total), $in.^3$	4200

TABLE I.- PHYSICAL CHARACTERISTICS OF BELL X-5 AIRPLANE

AT A SWEEP ANGLE OF 58.7° - Concluded

Vertical tail:	
Airfoil section (parallel to rear fuselage center line)	NACA 65A006
Area, sq ft	29.5
Span, perpendicular to rear fuselage center line, ft	6.25
Aspect ratio	1.32
Sweep angle of leading edge, deg	43
Fin:	
Area, sq ft	24.8
Rudder (23.1 percent overhang balance, 26.3 percent span):	
Area rearward of hinge line, sq ft	4.7
Span, ft	4.43
Travel, deg	±35
Chord, percent horizontal tail chord	22.7
Moment area rearward of hinge line, $in.^3$	3585

TABLE II.- RESULTS OF GROUND VIBRATION TESTS ON THE X-5 AIRPLANE

[Empty Weight]

Stabilizer Modes: (tests made with wing at 40° sweepback only)	
Stabilizer rocking coupled with fuselage torsion and fin bending, cps	15.9
Stabilizer rocking coupled with fin bending, cps	21.1
First symmetrical stabilizer bending coupled with fuselage vertical bending, cps	21.9
Symmetrical stabilizer rotation about its pivot axis coupled with stabilizer bending, cps	50.0
First antisymmetrical stabilizer bending, cps	58.0
First symmetrical stabilizer torsion, cps	75.9
First antisymmetrical stabilizer torsion, cps	79.1
Wing Modes: (test made with wing at 60° sweepback)	
First symmetrical wing bending, cps	10.3
First antisymmetrical wing bending coupled with fuselage modes, cps	16.0
First antisymmetrical wing torsion, cps	38.8
First symmetrical wing torsion, cps	39.4
Third antisymmetrical wing bending coupled with wing tip torsion, cps	58.3
Second symmetrical wing torsion, cps	65.6
Second antisymmetrical wing torsion coupled with wing bending, cps	66.0
Fuselage Modes: (tests made with wing at 60° sweepback)	
Fuselage side bending coupled with fuselage torsion and first symmetrical wing bending, cps	12.4
Fuselage vertical bending, cps	15.6
Fuselage torsion coupled with fuselage side bending, first antisymmetrical wing bending and stabilizer rocking, cps	16.0

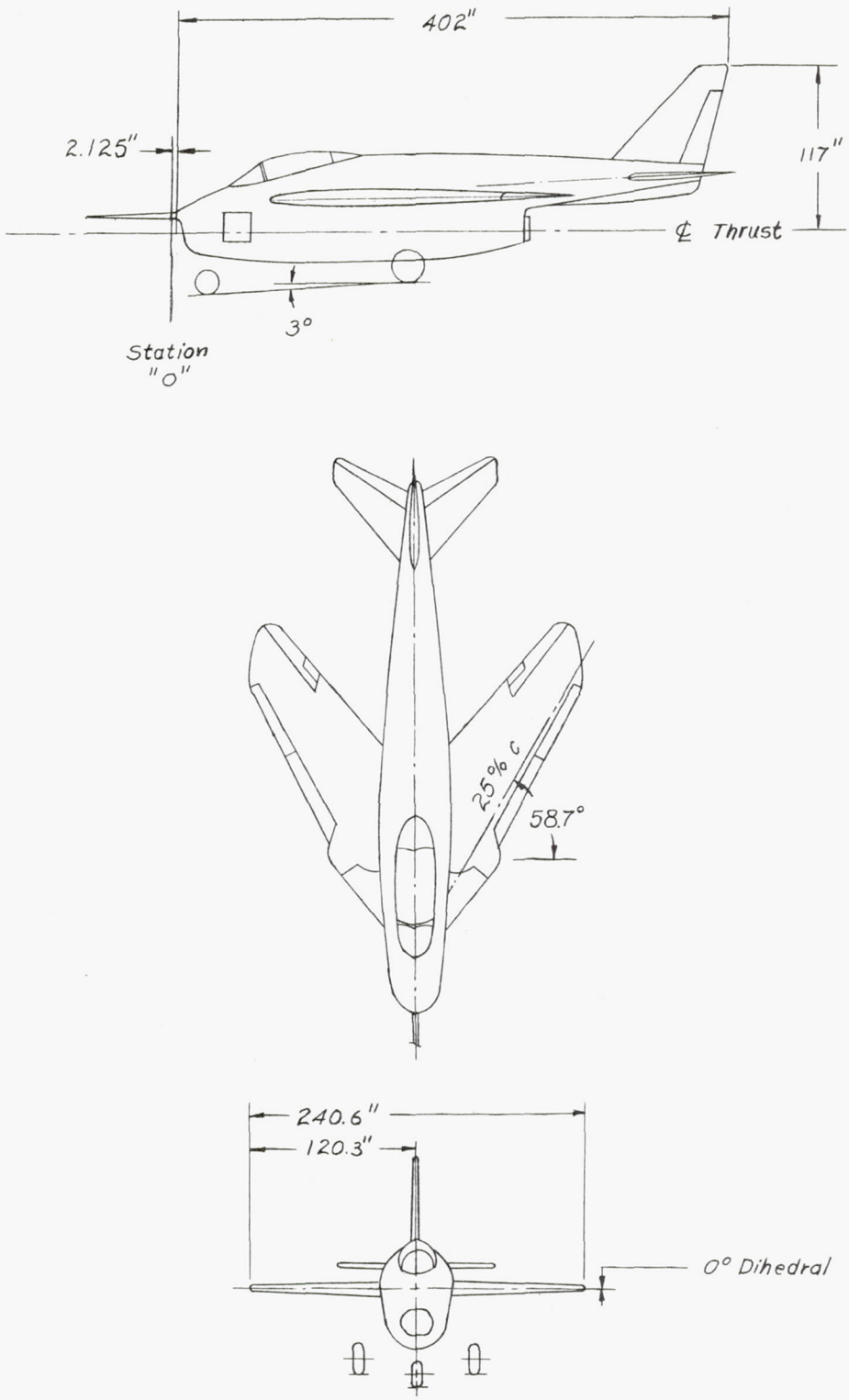

Figure 1.- Three-view drawing of the Bell X-5 research airplane at 58.7° sweepback.

LE-813

Figure 2.- Photograph of the Bell X-5 research airplane at 58.7° sweepback.

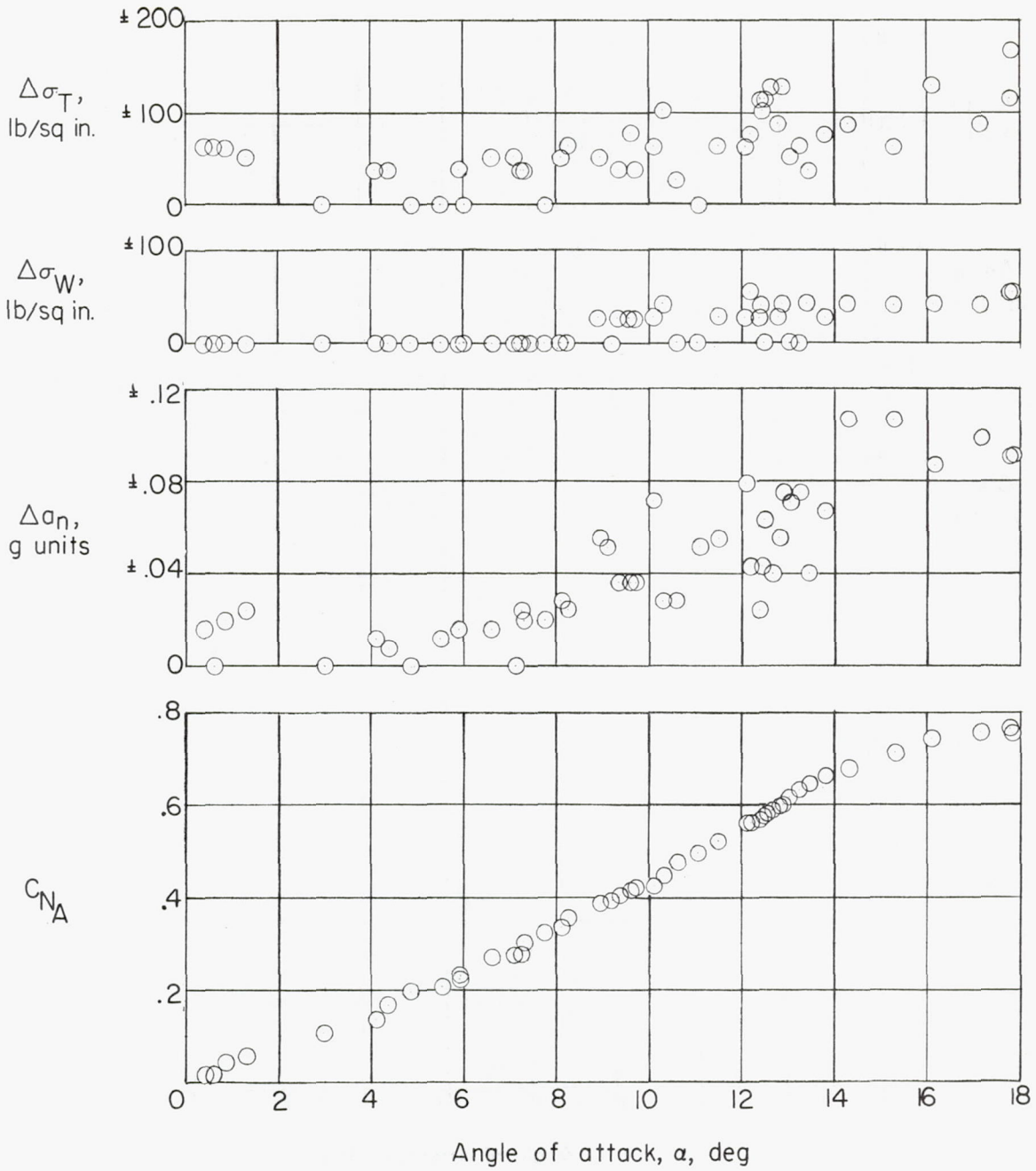

(a) M = 0.74 to 0.68; $h_p \approx 40{,}400$ feet; W = 8799 pounds.

Figure 3.- Typical variation of horizontal tail, wing, and airplane buffet parameters during push-over and pull-up maneuvers.

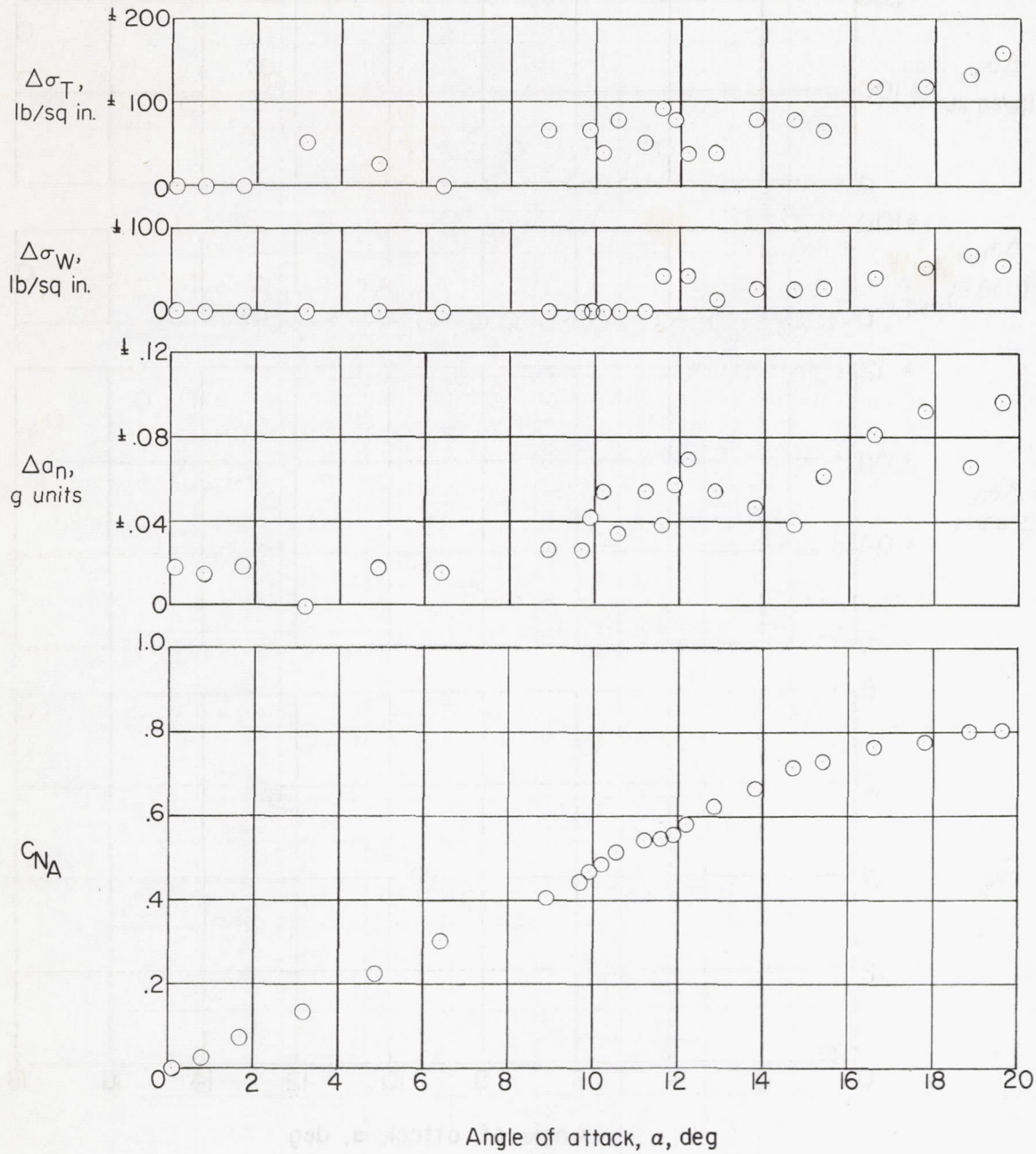

(b) M = 0.82 to 0.80; $h_p \approx 41{,}500$ feet; W = 8573 pounds.

Figure 3.- Continued.

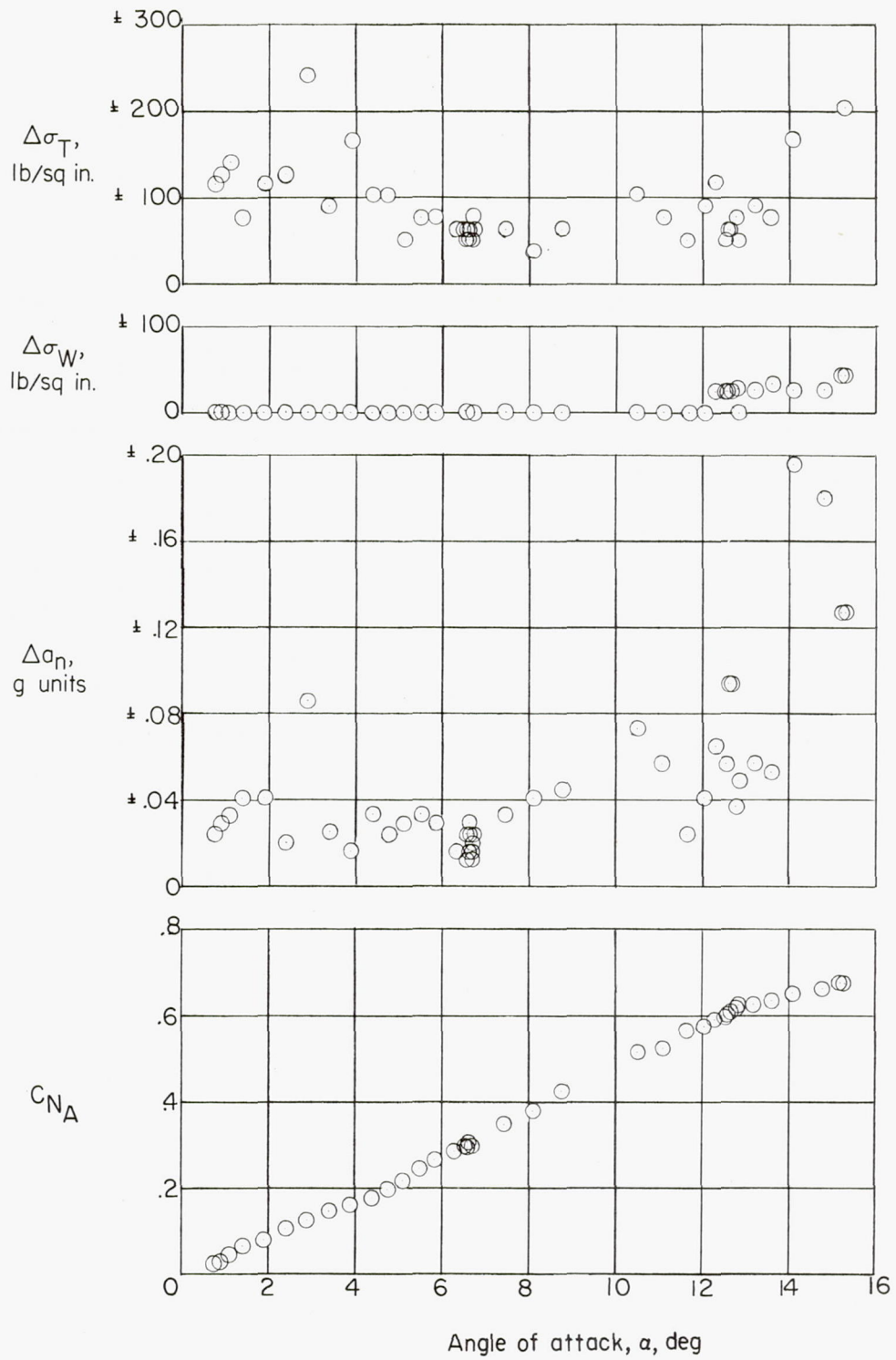

(c) M = 0.90 to 0.86; $h_p \approx 37{,}400$ feet; W = 8719 pounds.

Figure 3.- Continued.

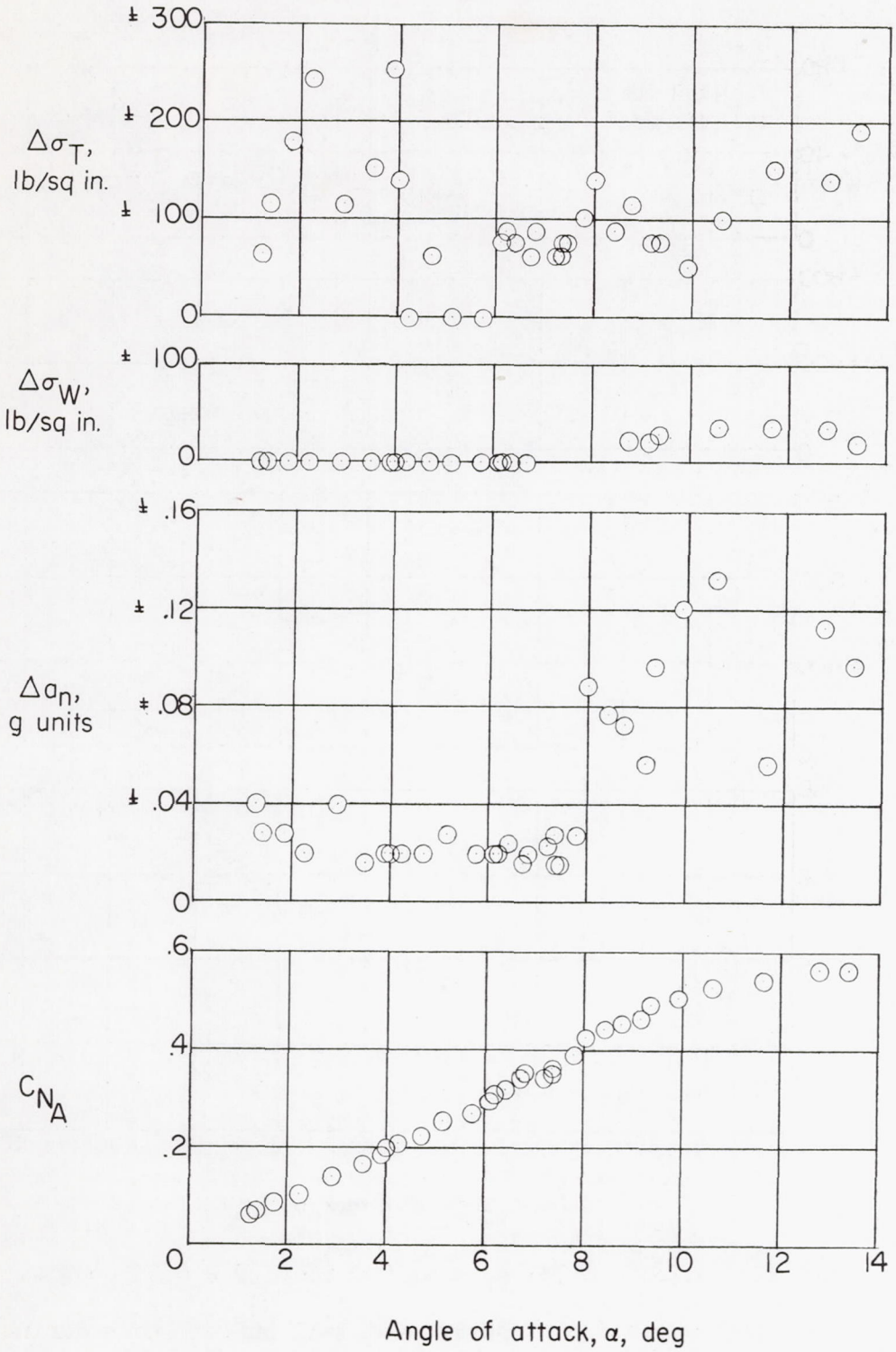

(d) M = 0.97; $h_p \approx 38{,}500$ feet; W = 8562 pounds.

Figure 3.- Concluded.

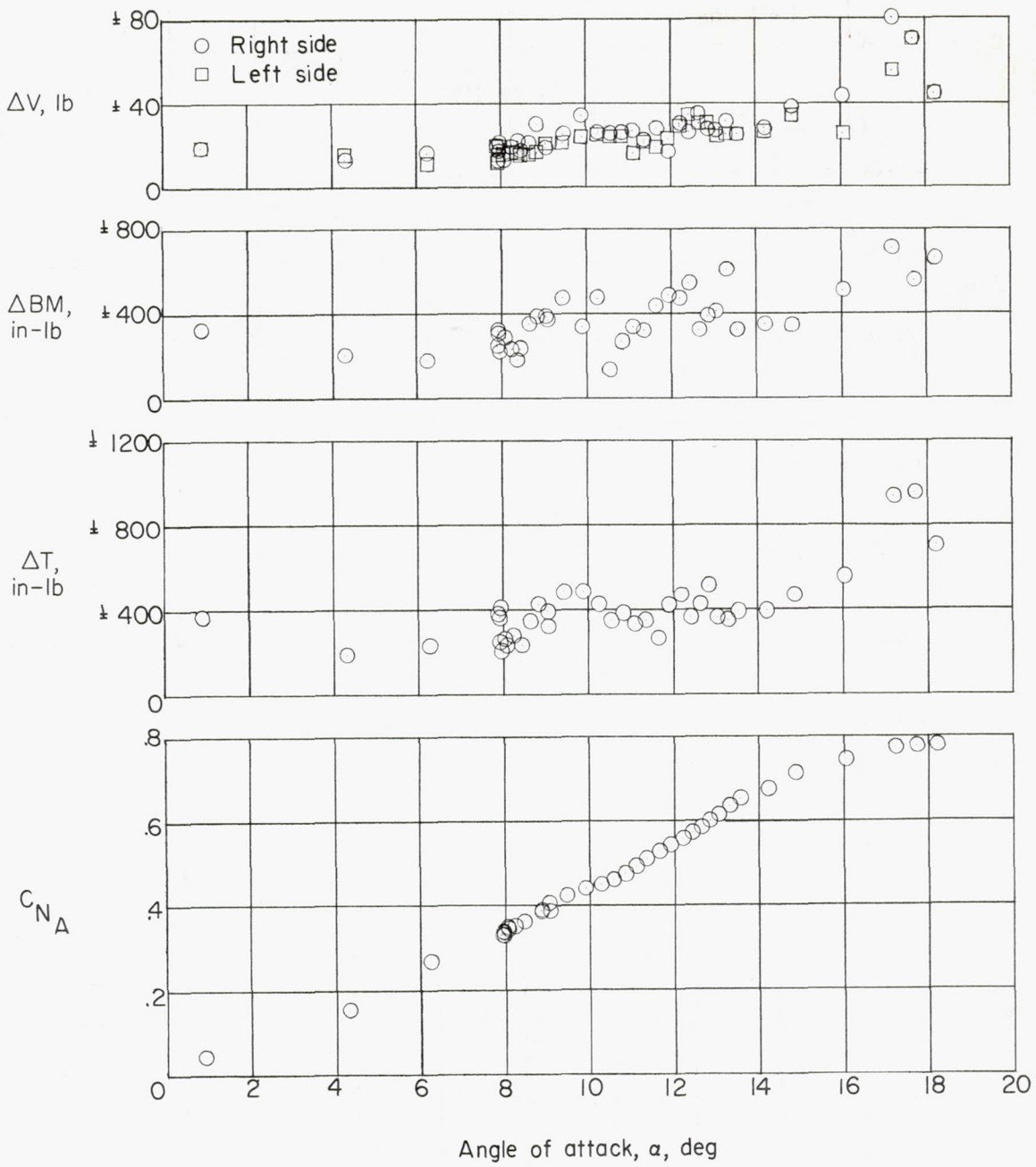

(a) M = 0.76 to 0.73; $h_p \approx 41{,}000$ feet; W = 8863 pounds.

Figure 4.- Typical variation of horizontal tail buffet loads during push-over and pull-up maneuvers.

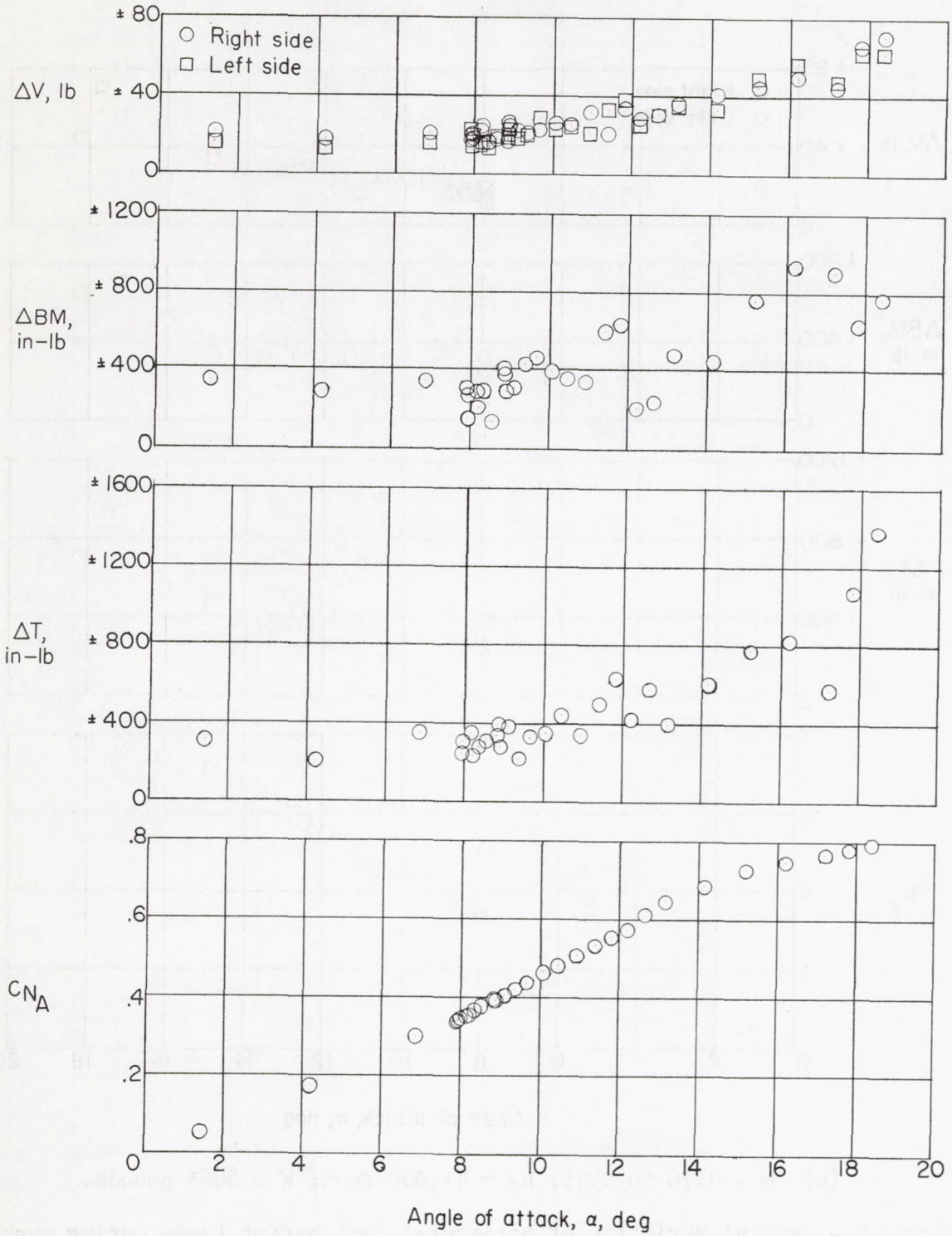

(b) M = 0.82 to 0.79; $h_p \approx 39{,}600$ feet; W = 8837 pounds.

Figure 4.- Continued.

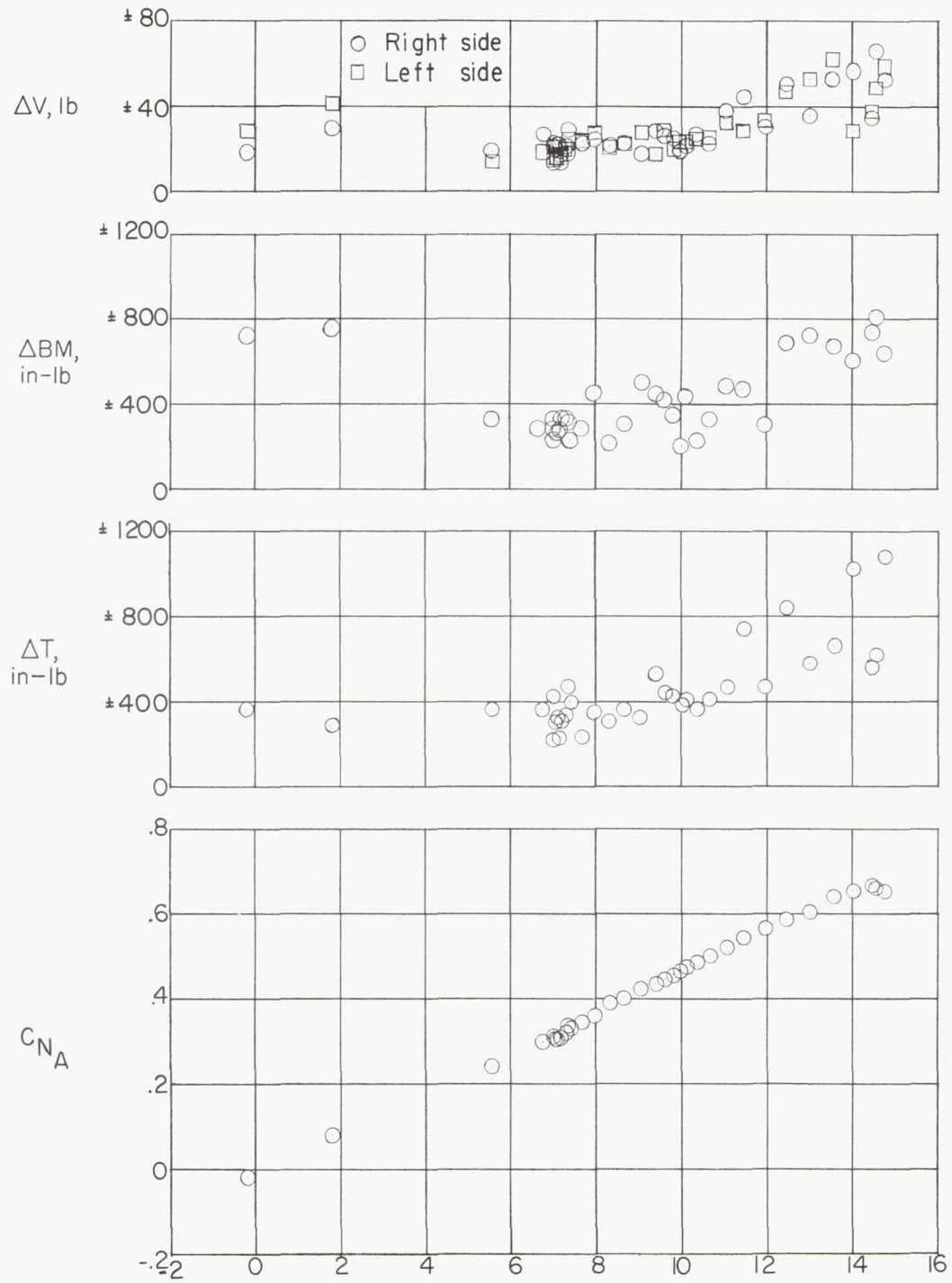

(c) M = 0.87 to 0.85; $h_p \approx 38{,}500$ feet; W = 8805 pounds.

Figure 4.- Continued.

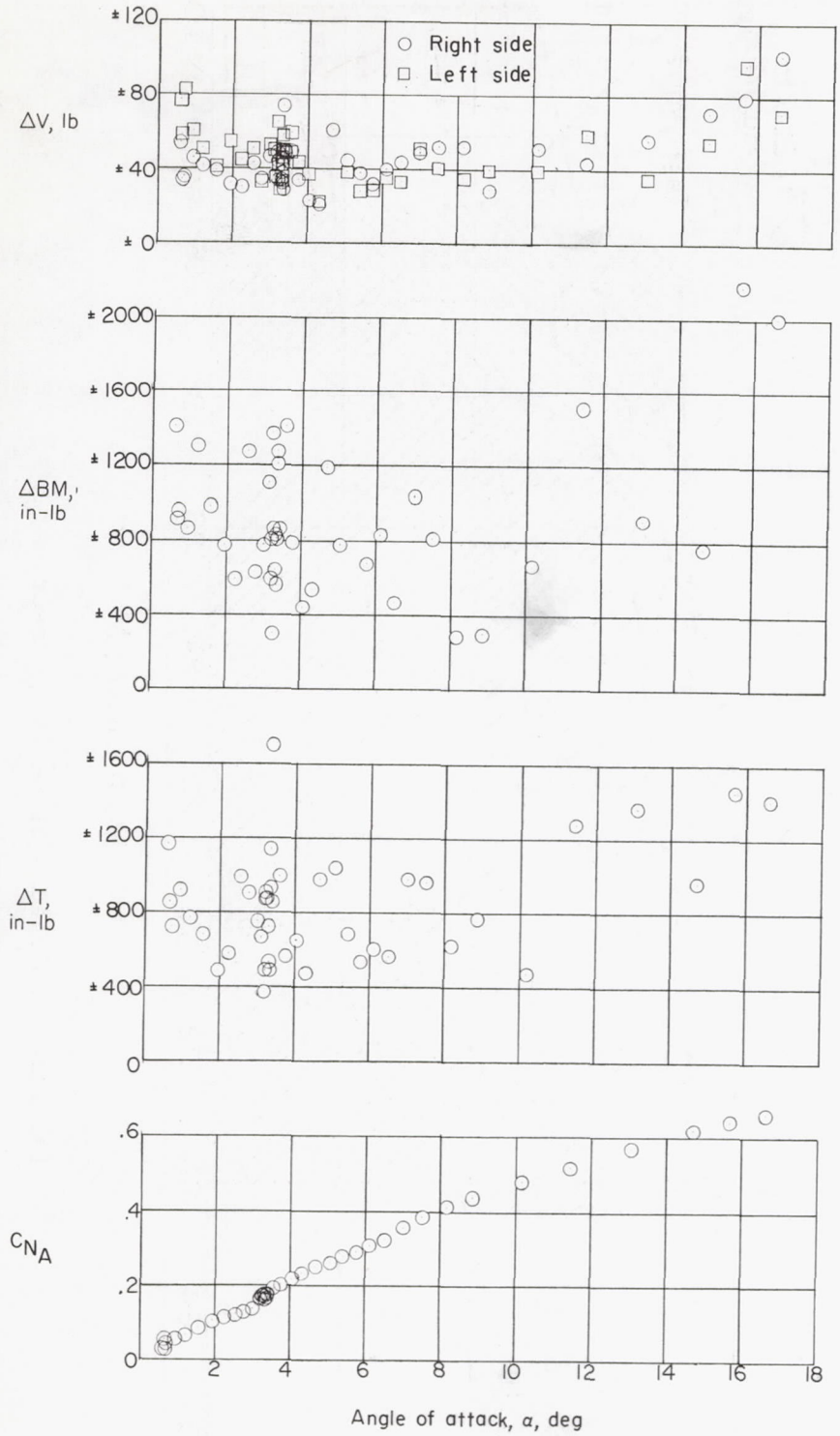

(d) M = 0.96 to 0.93; $h_p \approx 37,600$ feet; W = 8644 pounds.

Figure 4.- Concluded.

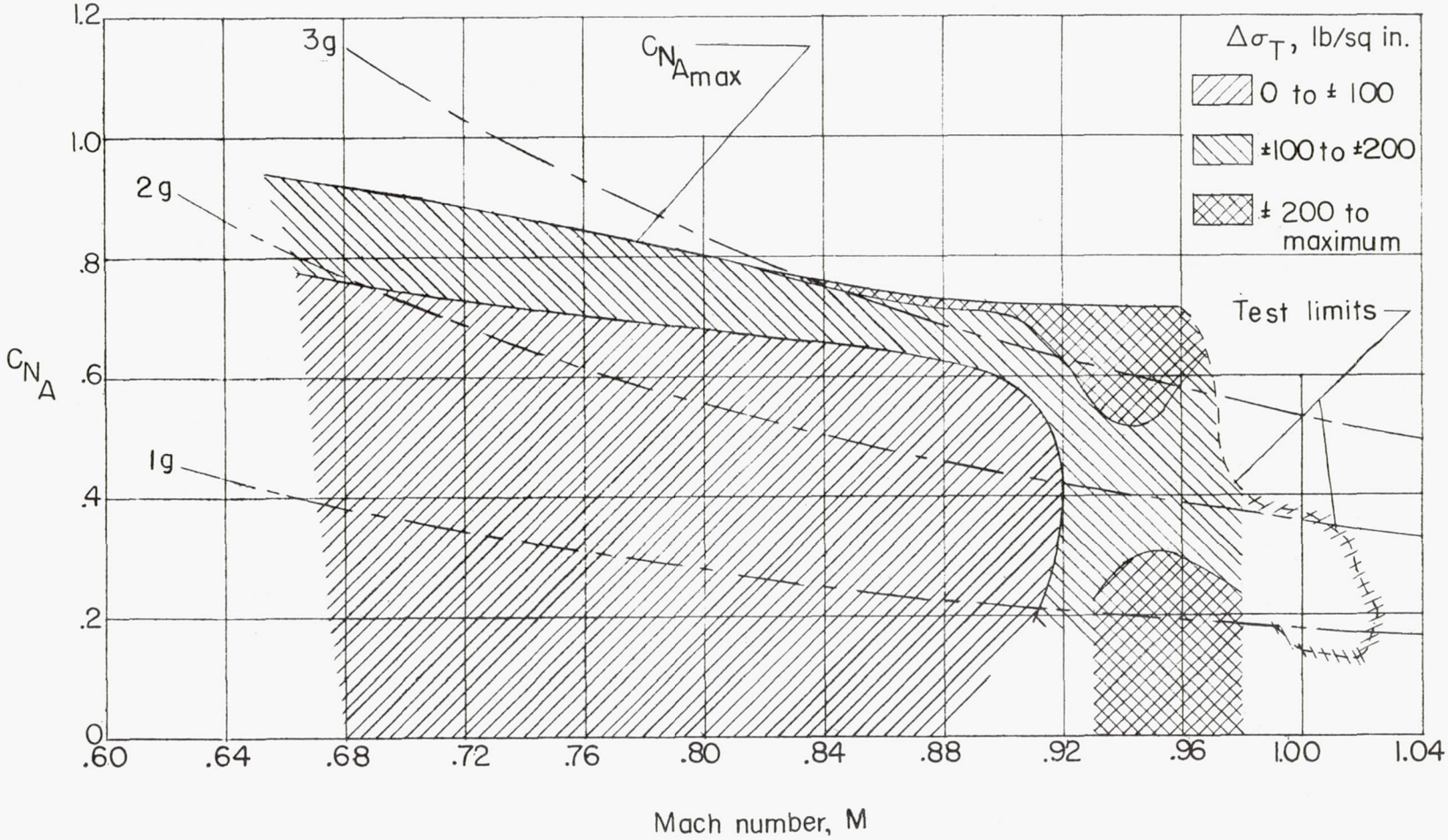

(a) Buffet-induced tail bending stress $\Delta\sigma_T$.

Figure 5.- Summary of tail buffet intensities encountered by the Bell X-5 research airplane at an altitude of approximately 40,000 feet.

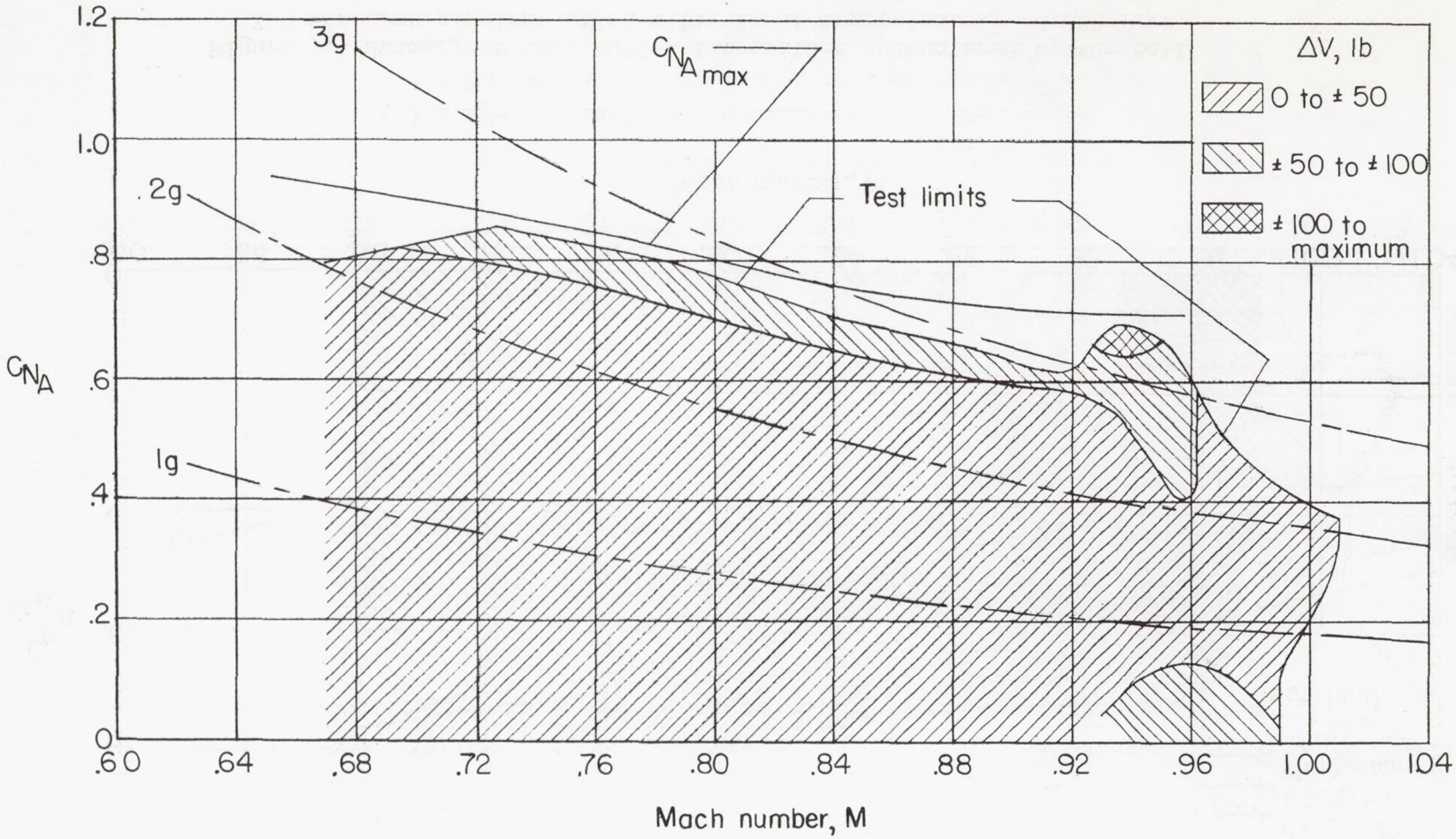

(b) Buffet-induced tail shear load, right side, ΔV.

Figure 5.- Continued.

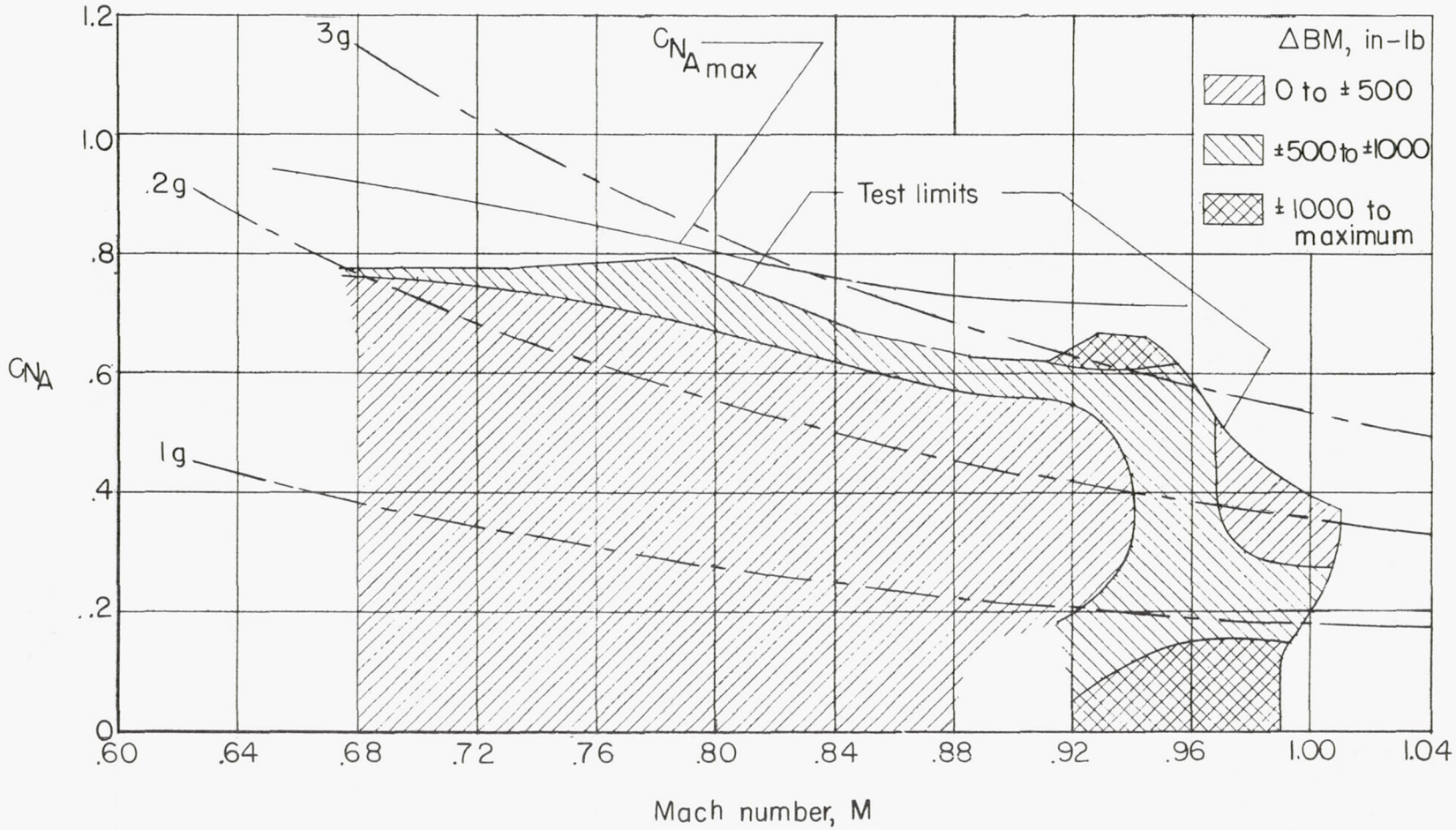

(c) Buffet-induced tail bending moment ΔBM.

Figure 5.- Continued.

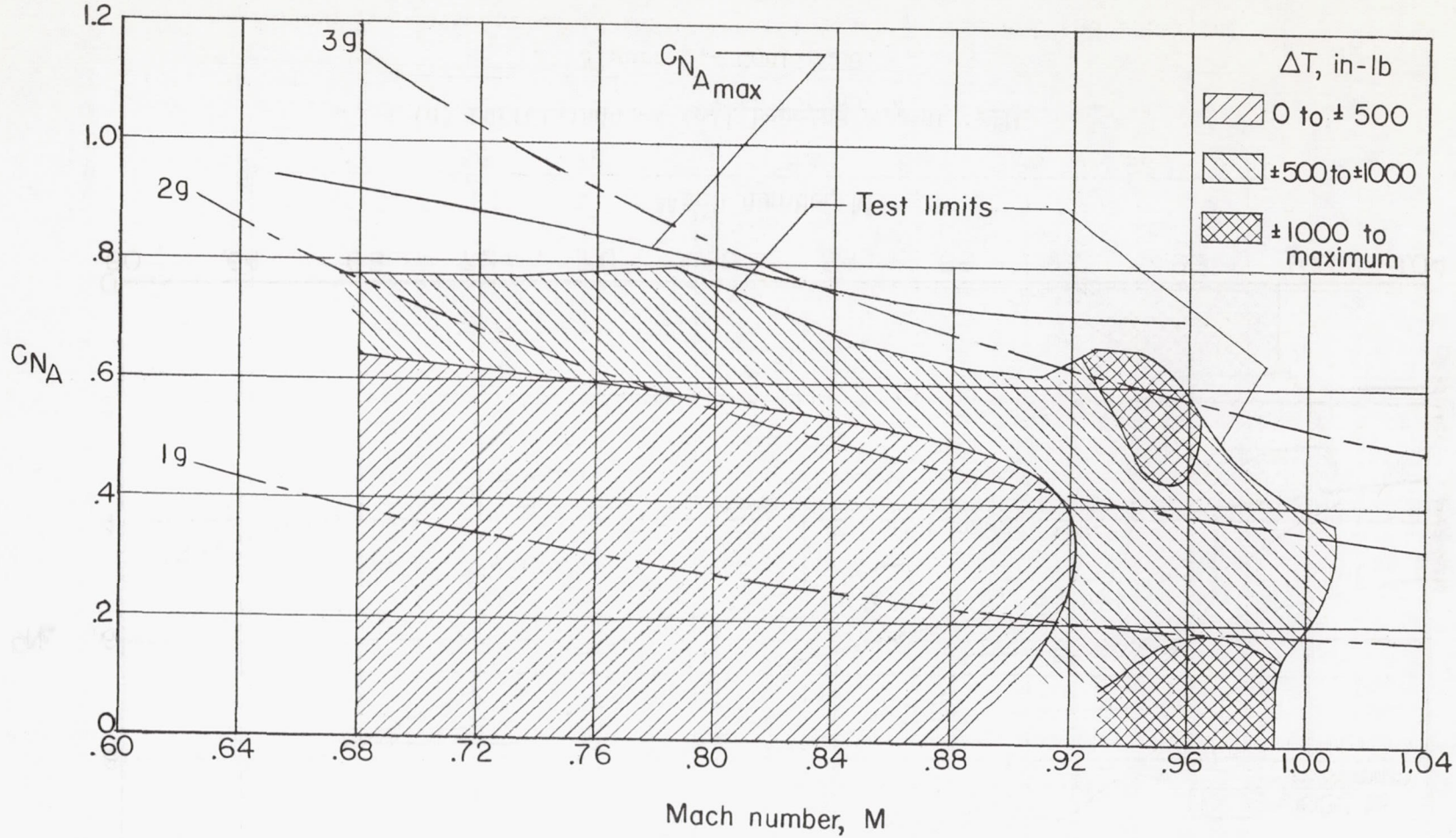

(d) Buffet-induced tail torque ΔT.

Figure 5.- Concluded.

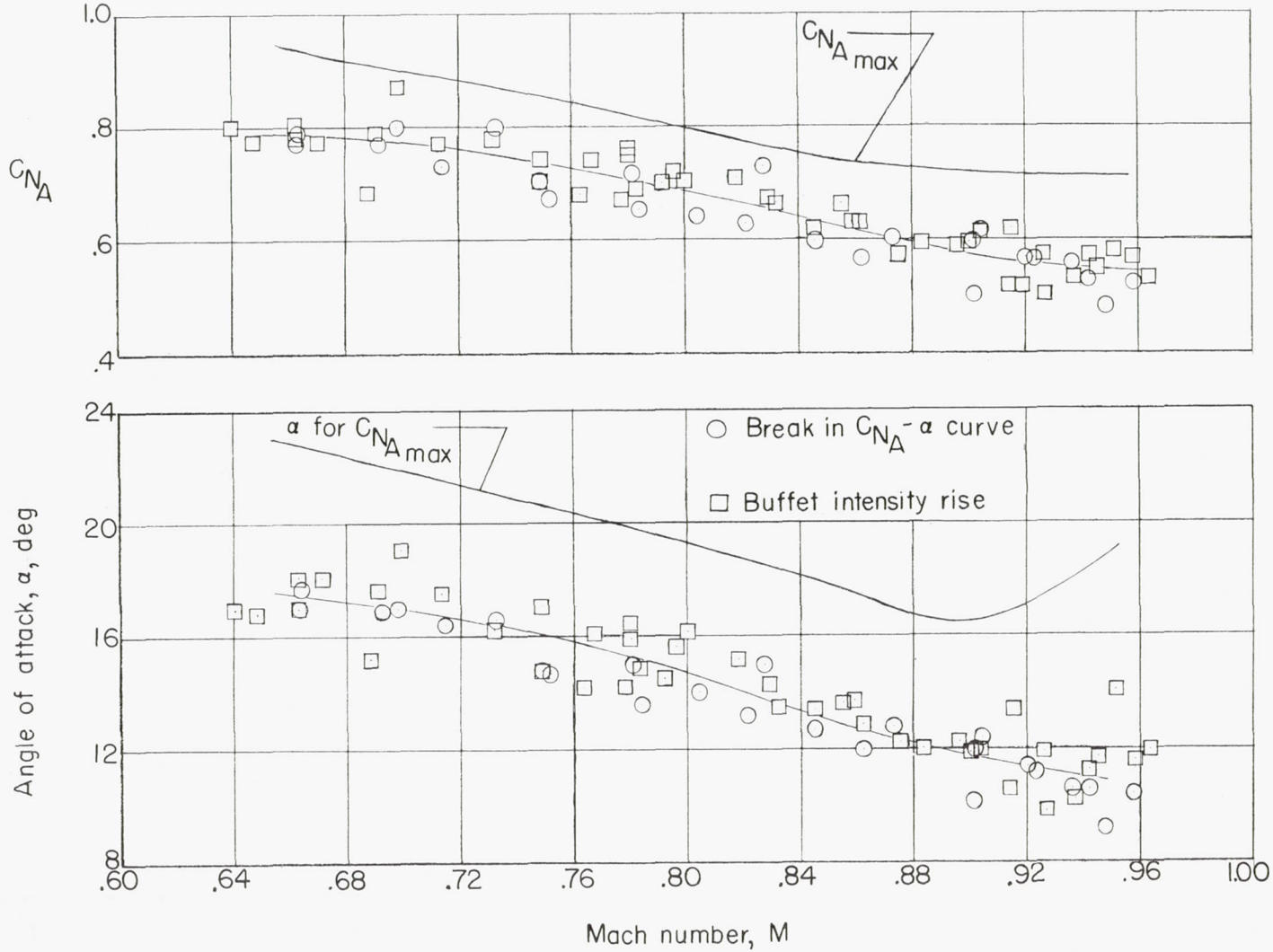

Figure 6.- Correlation of tail buffet intensity rise and the break in C_{N_A} - α curve.

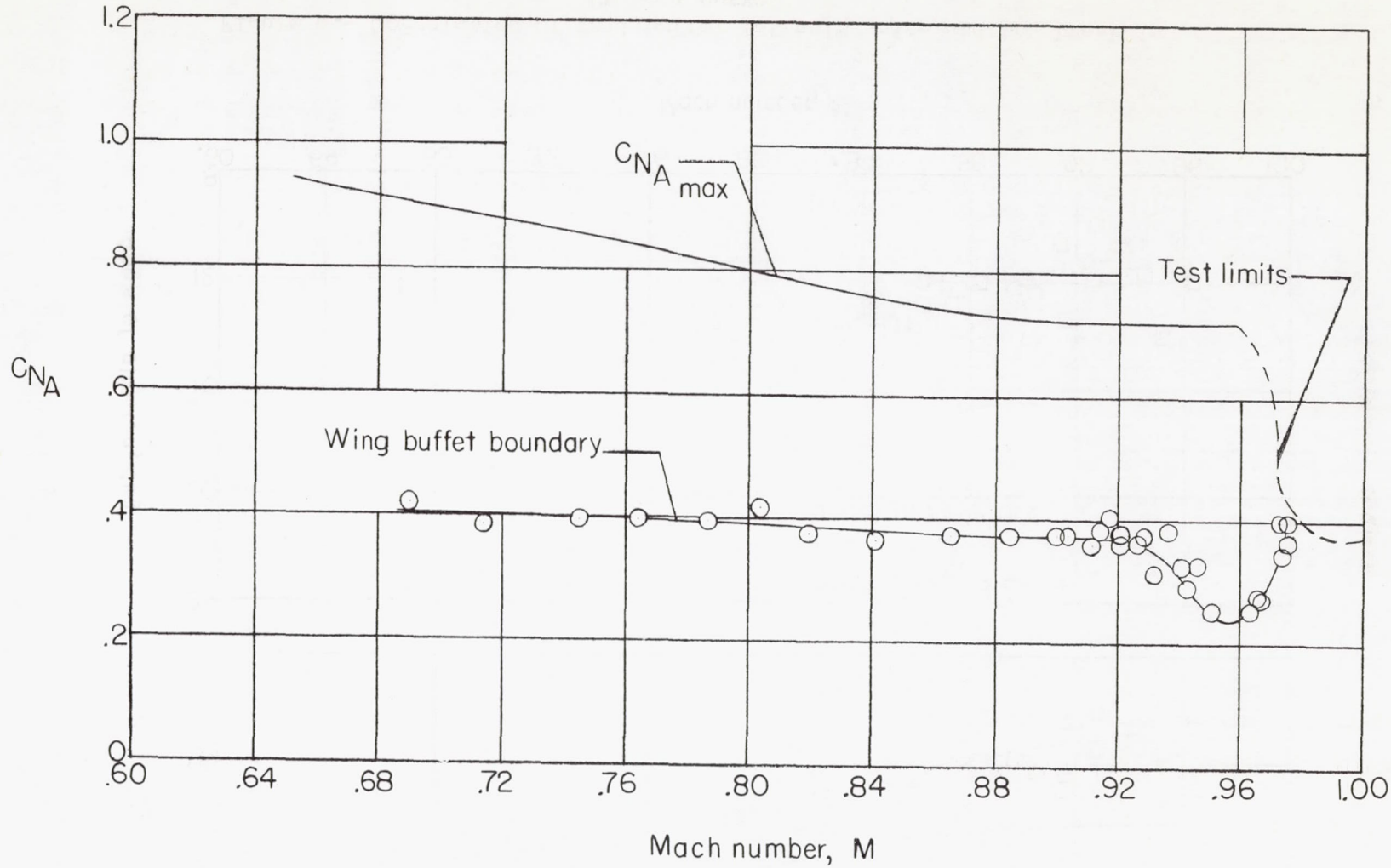

Figure 7.- Wing buffet boundary of the Bell X-5 research airplane.